Investigating the Sensitivity of Glacier Mass-Balance/Elevation Profiles to Changing Meteorological Conditions: Model Experiments for Haut Glacier D'Arolla, Valais, Switzerland

Author: Arnold, Neil

Source: Arctic, Antarctic, and Alpine Research, 37(2) : 139-145

Published By: Institute of Arctic and Alpine Research (INSTAAR), University of Colorado

URL: https://doi.org/10.1657/1523-0430(2005)037[0139:ITSOGE]2.0.CO;2

Arctic, Antarctic, and Alpine Research, Vol. 37, No. 2, 2005, pp. 139–145

Investigating the Sensitivity of Glacier Mass-Balance/Elevation Profiles to Changing Meteorological Conditions: Model Experiments for Haut Glacier D'Arolla, Valais, Switzerland

Neil Arnold

Scott Polar Research Institute,
University of Cambridge,
Lensfield Road, Cambridge, CB2 1ER,
United Kingdom.
nsa12@cam.ac.uk

Abstract

This paper presents the results of a distributed surface energy balance model which is used to calculate season-long patterns of melt on a small valley glacier, Haut Glacier d'Arolla, Valais, Switzerland, under different summer meteorological conditions and winter snow depth distributions. The model uses a Digital Elevation Model of the glacier and the surrounding topography, together with meteorological data collected at a site in front of the glacier to determine hourly totals of the surface energy balance components, and hence melt, over the entire glacier surface throughout a melt season, with a spatial resolution of 20 m. From these results, the spatially averaged mass-balance/elevation profile for the glacier can be calculated. A cubic relationship with elevation gives the best fit to the calculated mass-balance curve. The shape of this profile varies with the imposed change in meteorological conditions, however, becoming increasingly "S" shaped for warmer or less snowy conditions. These mass-balance profile changes are due to the complex interplay between albedo variations due to different snow depths over the glacier surface (and eventual removal of the snow cover), the variations in solar energy receipts caused by slope and aspect variation over the glacier and the changing patterns of shading by the surrounding topography. The changes in mass-balance profile lead to maximum calculated mass-balance sensitivity to imposed change occurring at intermediate elevations on the glacier; the calculated equilibrium-line altitude (ELA) occurs at the upper end of this zone, resulting in very large calculated changes in the ELA for different climatic conditions.

Introduction

The mass-balance/elevation profile of any given glacier can be calculated from the elevation gradient of snowfall minus that of surface melt. The amount of melt produced depends on the surface energy balance. This, in turn, depends on a complex interplay between surface conditions on the glacier, external meteorological factors, and the topography of the glacier surface itself and the surrounding areas. This complexity has meant that mathematical models of these factors have been an important technique for understanding and simulating patterns of surface melt. Models of glacier mass and energy balance range from simple 0- or 1-dimensional statistical relationships between meteorological factors and measured mass balance (e.g., Willis et al., 1993), through degree-day type approaches (e.g., Laumann and Reeh, 1993; Braithwaite and Zhang, 2000) and 0-dimensional (at-a-point) or 1-dimensional (center-line) energy balance studies (e.g., Braithwaite and Olesen, 1990; Munro, 1990; Oerlemans, 1993), to sophisticated 2-dimensional spatially-distributed, physically based models (e.g., Munro and Young, 1982; Escher-Vetter, 1985; Arnold et al., 1996; Hock and Noetzli, 1997; Brock et al., 2000a). Such models generally calculate the retreat of the summer snowline in order to allow for the different surface properties (such as albedo and aerodynamic roughness) of snow, ice, and firn.

Only the final approach can produce estimates of the spatial and temporal variability of melt across a glacier surface, and throughout an ablation season (Brock et al., 2000a). Such a model should therefore be a more effective tool than the simpler models for calculating the variation in melt rates with elevation, and hence (given a knowledge of snowfall amounts) the mass-balance/elevation profile of any given glacier in a given year. Given their ability to track the changes in surface type over the course of a melt season, 2-dimensional models should also provide improved estimates of the possible change in glacier mass-balance profiles under changing climatic conditions.

In this paper I use the model developed by Arnold et al. (1996), with the improvements incorporated by Brock et al. (2000a), in a series of sensitivity analyses using changing summer temperatures and winter snow depths to investigate how the modeled yearly mass-balance/elevation profile at Haut Glacier d'Arolla (Fig. 1) varies under different climatic conditions. Haut Glacier d'Arolla is a small, north-facing valley glacier, approximately 6 km^2 in area, located in Valais in the southwestern Swiss Alps.

Methods

THE SURFACE ENERGY-BALANCE MODEL

The model assumes that there are four main components of the surface energy balance; short-wave (solar) radiation; long-wave (terrestrial) radiation; sensible turbulent heat; and latent turbulent heat. These four components are calculated for each grid cell of the Digital Elevation Model (DEM) every hour of the melt-season using the measured meteorological data and calculated solar altitude and azimuth.

Shortwave radiation is generally acknowledged to be the most important of these, especially for temperate glaciers, (e.g., Munro and Young, 1982), and is treated in the most detail. The model uses measured incoming shortwave radiation data from a meteorological station located within the catchment of the glacier (Fig. 1). This is then

1523-0430/05 $7.00

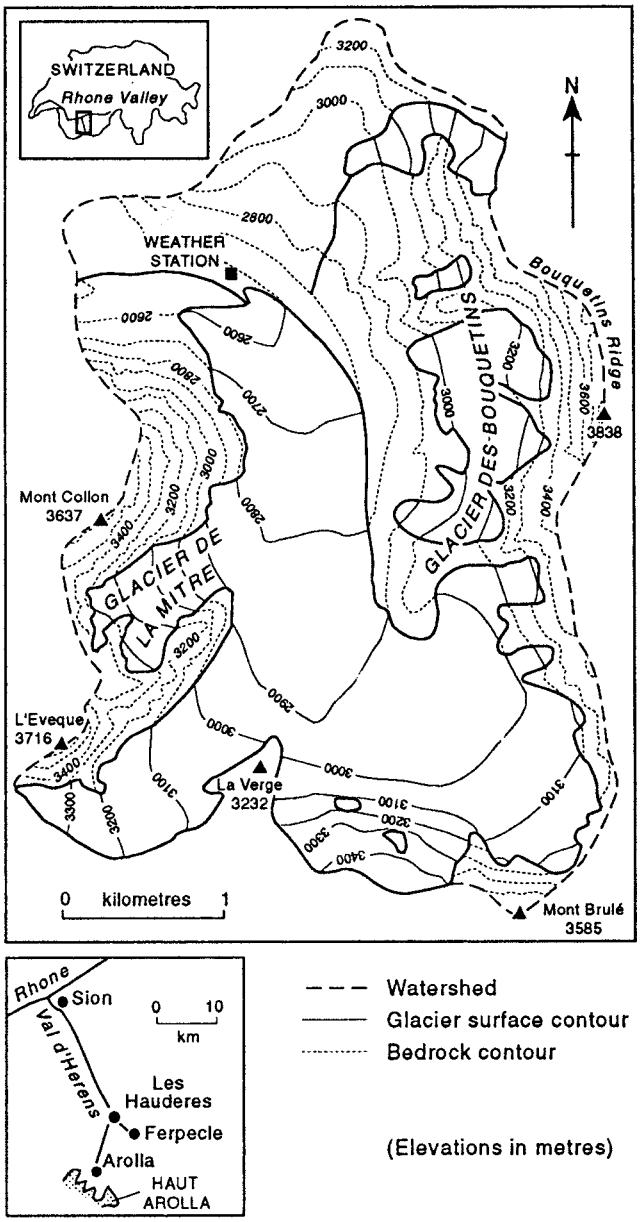

FIGURE 1. Location map of Haut Glacier d'Arolla, showing the location of the weather station and topographic features discussed in the text.

modified by the slope and aspect of the glacier in each grid cell to give the incoming direct solar radiation for each cell. If a cell is shaded by the surrounding topography, however, it is assumed to only receive diffuse radiation, which is assumed to be 20% of the measured direct radiation, following Oerlemans (1993). This is supplemented by reflected radiation from the surrounding topography, calculated using a view factor relationship (Munro and Young, 1982). From these values for incoming radiation, the net solar radiation is calculated using the surface albedo of the grid cell in question at the time. The albedo is calculated using the parameterizations developed by Brock et al. (2000b). The main control is the presence of snow or ice in a grid cell; the albedo of snow decreases with accumulated daily maximum temperature, which was found to act as a surrogate for the evolution of snow grain size, one of the key controls on albedo (Brock et al., 2000b). Ice albedo is assumed to increase slowly with increasing elevation.

The model assumes that the surface of the glacier is always at 0°C, so outgoing longwave radiation is constant. Incoming longwave radiation is calculated using the relationships described by Braithwaite and Olesen (1990) which depend on the measured air temperature and cloud amount (which in this study was derived from the daily measured temperature range [Arnold et al., 1996]).

To calculate the turbulent fluxes, measured air temperature at the weather station is used together with an assumed lapse rate of 6.5°C km^{-1} to calculate the air temperature in each grid cell. Relative humidity and wind speed are assumed to be constant over the catchment, and a lapse rate of 10 kPa km^{-1} is used to calculate air pressure over each DEM cell. From these input data, an iterative scheme is used to calculate the Obhukov length scale (Munro, 1990), and from this the sensible and latent heat fluxes. These equations require the surface roughness length scale to be known; these are calculated using the relationships derived by Brock et al. (2000b).

The four components, as calculated for each DEM cell for each hour, are added together and if the result is positive, melt is assumed to occur in that cell at that time. Any measured precipitation (assumed to be uniform over the catchment) for a time step is assumed to fall as snow if the temperature in any given grid cell is below 1°C; this is deducted from any calculated melt for that grid cell.

STUDY AREA AND DATA REQUIREMENTS

Haut Glacier d'Arolla has been the subject of ongoing research in glacier mass and energy balance, hydrology, geochemistry, and dynamics since the early 1990s (e.g., Sharp et al., 1993; Arnold et al., 1996; Richards et al., 1998; Brock et al., 2000a, 2000b; Willis et al., 2002). It is a small (approximately 6 km^2), north-facing valley glacier in the southwestern Swiss Alps. The glacier has been retreating in the latter half of the 20th century (Oerlemans et al., 1998). The climate in the area is temperate, with warm summers, and cold, fairly wet winters, although this general pattern is strongly affected by local relief.

Data requirements for the model used here can be broadly divided into those required to drive the model as model inputs, and those required for validation. The model requires four main input datasets. A detailed description of the methods used to obtain these data is given in Arnold et al. (1996), but briefly they comprise (1) a 20-m resolution Digital Elevation Model (DEM) of the glacier surface, and the surrounding topography, obtained by a combination of surveying for the glacier surface itself, and contour data from Swiss National Survey 1:25000 topographic maps for the surrounding areas; (2) solar altitude and azimuth data, calculated using standard astronomical theory (e.g., Walraven, 1978); (3) initial snow-cover data in water equivalent units, obtained from early-season measurements of snow depth and density at various locations over the glacier surface, and (4) meteorological data collected every 10 min, then averaged hourly, by an automatic weather station at a site 100 m in front of the glacier (see Fig. 1 for location). From (1) and (2) the model calculates patterns of shading, and surface slope and aspect, which affect shortwave radiation receipts; (3) allows initial albedo patterns to be established, which again affect absorption of short-wave radiation; and (1) and (4), together with standard lapse rate and elevation/pressure relationships, allow the turbulent fluxes for each cell in the DEM to be calculated.

Data for model validation are also described in more detail in Arnold et al. (1996) and Brock et al. (2000a, 2000b). Briefly, the model has been validated using intensive summer measurement programs of daily melt rates at a network of stakes drilled into the glacier surface; patterns of summer snow-line retreat; and patterns of surface albedo (Arnold et al., 1996; Brock et al., 2002a, 2000b). The calculated hourly melt has also been compared with hourly measurements of melt made with an ultrasonic depth gauge located on the glacier surface (Willis et al., 2002).

MODEL EXPERIMENTS

The model experiments in this study are based on meteorological and snow-depth data from 1990, as used in Arnold et al. (1996). The summer melt season is assumed to extend from 30 May to 23 August (the period of meteorological data availability). Data from other years suggests that the first snowfall of the autumn typically occurs in late August or early September (e.g., Arnold et al., 1998). After this, melt reduces dramatically. Although the first snowfall event for 1990 was not recorded, daily ablation amounts in other years at this time are typically ~10 mm water equivalent (w.e.) per day, compared with peak melt rates of over 50 mm w.e. per day, and season-long melt totals of 2.5 to 4.8 m w.e. Thus, 1 or 2 extra weeks of melt would only add perhaps 100 to 200 mm w.e. of melt, and would not change the overall results significantly.

The sensitivity experiments undertaken in this study focus on the effect of changing summer temperature and winter snowfall from these reference values. In the tests, summer temperatures as measured at the meteorological station are varied by −2°C, −1°C, −0.5°C, +0.5°C, +1°C, and +2°C, and winter snow depths are changed by −20%, −10%, −5%, +5%, +10%, and +20%. The combination of these (together with the "standard" run using the measured temperature and snow depth for 1990) results in a set of 49 different runs.

POSTPROCESSING

The spatially distributed results for the 49 model runs are summarized by calculating a mean mass-balance value for 87, 10-m elevation-change bands over the glacier surface (calculated by taking the sum of winter snow depth or total modeled summer melt of all DEM cells within the elevation band, and dividing by the number of cells in the band), to produce a spatially averaged mass-balance/elevation profile for the different experiments. The mass balance is assumed to be the late-winter snow depth at the start of the modeled melt-season, minus the modeled summer melt. This approach obviously does not directly take into account melt which occurs outside the summer period (except that such melt would reduce the late-winter snow depth), but it does allow for summer snowfall events, as these are accounted for in the model, as discussed above. These profiles differ from the modeled center-line mass-balance profile, as the center-line profile does not allow for the generally lower melt values near the sides of the glacier, due to the increased shading at the sides by the surrounding topography. The impact of this effect is discussed below.

Model Results

The validation and testing of the model is described in Arnold et al. (1996). The performance of the improvements to turbulent fluxes, and the albedo and roughness parameterizations are discussed in Brock et al. (2000a). In general, the model was very successful. The model accurately predicted the measured snowline elevation during 1990 ($r =$ 0.98); measured daily ablation at a series of center-line ablation stakes ($r = 0.84$), and measured surface albedo ($r = 0.83$). The mean difference between modeled and measured daily ablation totals was 0.3 mm w.e. per day. The model also performs well at an hourly resolution; the correlation between hourly modeled and measured ablation on the glacier was 0.86 (Willis et al., 2002).

Calculated center-line mass-balance values are on average 0.12 m w.e. more negative than the areally averaged values (i.e. melt is being over-estimated), the equivalent of approximately 700,000 m^3 of extra melt if center-line values are used to estimate glacier-wide melt rates. The difference between center-line and areally averaged mass-balance values varies with elevation, however; allowing for glacier hypsometry produces a difference of over 800,000 m^3 of melt. This is the equivalent of over 8% of the total calculated melt production.

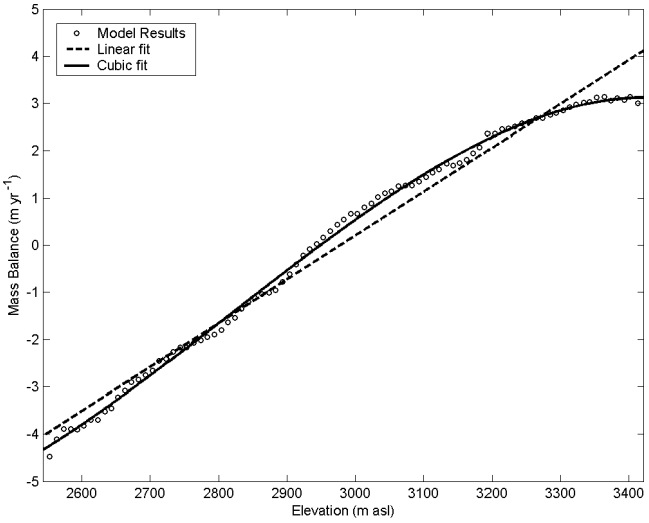

FIGURE 2. Mass-balance/elevation profile for the standard run, averaged over the glacier surface by 10-m elevation-change bands. Open circles: model results; dashed line: best-fit linear relationship; solid line: best-fit cubic relationship.

The calculated areally averaged mass-balance/elevation profile for the standard run is shown in Figure 2. As expected, there is a strong trend for increasing mass-balance at higher elevations. A fitted linear elevation/mass-balance relationship (Fig. 2, dashed line) shows a high R^2 value of 0.981, but the residuals from the relationship are not normally distributed; the fitted relationship overestimates mass balance at both low and high elevations, and underestimates the mass balance at intermediate elevations. This suggests that a nonlinear relationship will describe the mass-balance/elevation profile more effectively. A cubic relationship (Fig. 2, solid line) is the lowest-order polynomial relationship which gives a normal distribution of residuals, and has an R^2 value of 0.998. This form of relationship allows for the lower mass-balance/elevation gradient at low and high elevations, and the steep gradient in the central section of the glacier. The second derivative of the fitted cubic relationship shows that the maximum mass-balance/elevation gradient occurs at 2820 m.

The best-fit cubic mass-balance profiles (solid lines) for the eight most extreme sensitivity experiments, together with the best-fit profile for the standard run (dashed lines), are shown in Figure 3. At first glance, the results seem straightforward. Larger winter snow depths or lower summer temperatures lead to a less negative mass balance at any given elevation, and vice versa. However, the impact of the changes does not occur uniformly with elevation. Changing winter snow depth alone has a larger impact at higher elevations (e.g., Fig. 3d, f) than at lower elevations, whereas the impact of temperature alone seems to be largest at intermediate elevations (~2600 to ~3000 m, e.g., Fig. 3b, h).

As well as these changes in mass balance at different elevations, the shape of the mass-balance profile also alters markedly. For colder and/or snowier runs, the mass-balance profile is convex-up throughout the elevation range (d^2y/dx^2 is negative at all modeled elevations, e.g., Fig. 3a, b). For these runs, a quadratic relationship fits the model results as well as a cubic relationship. As winter snow decreases, or summer temperatures increase, a cubic relationship becomes the lowest order polynomial which fits the data; the best-fit profile becomes increasingly S shaped with warmer temperatures or lower snow depths, with d^2y/dx^2 changing from positive to negative at some intermediate elevation (between ~2800 m and ~3000 m, e.g., Figure 3h, i). The elevation at which d^2y/dx^2 is zero for the 49 model experiments is given in Table 1.

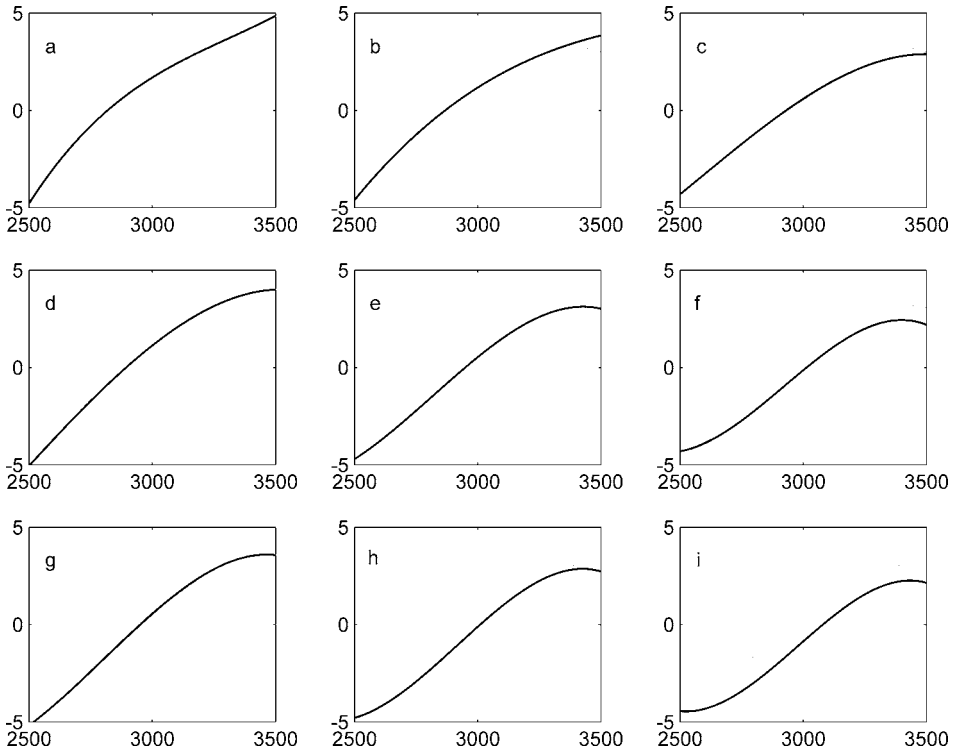

FIGURE 3. Best-fit cubic relationships for nine sensitivity experiments. a = Snow + 20%, T − 2°C; b = Snow + 0%, T − 2°C; c = Snow − 20%, T − 2°C; d = Snow + 20%, T + 0°C; e = Snow + 0%, T + 0°C (standard run); f = Snow − 20%, T + 0°C; g = Snow + 20%, T + 2°C; h = Snow + 0%, T + 2°C; i = Snow − 20%, T + 2°C. Horizontal axis is elevation (m a.s.l.); vertical axis is mass balance (m yr^{-1}). The dashed line in all figures except (e) is the mass balance profile for the standard run.

For the colder, snowier runs, with a convex-up profile, no clear trend can be seen, but for the runs with an obvious S-shaped curve (shown in bold in Table 1), a clear pattern emerges; the elevation of maximum mass-balance/elevation gradient moves upglacier with increasing summer temperature and decreasing winter snow depth. These variations lead to the largest changes in mass balance occurring at these intermediate elevations on the glacier—the zone of high potential solar radiation receipt.

The equilibrium-line altitude (ELA) for Haut Glacier d'Arolla is calculated to be at the upper end of this zone of high mass-balance sensitivity (Table 2). The changes in the shape of the mass-balance profile give rise to large changes in the calculated position of the ELA in the various model runs; the difference in ELA between the two most extreme runs (snow + 20%, T − 2°C; and snow − 20%, T + 2°C) is almost 280 m. This results in a large change in the accumulation area ratio (AAR), from 0.475 for the standard run (just below the range for steady-state mid-latitude glaciers of 0.5 to 0.8 (Porter, 1975), and thus in broad agreement with the observed retreat of the glacier since 1989), to 0.75 for the snow + 20%, T − 2°C run, to 0.18 for the snow − 20%, T + 2°C run.

The different effects of winter snow depth and summer temperature also mean that an apparent similarity in calculated ELA taken in isolation can in fact mask a large change in the calculated profile. The calculated ELAs for the snow − 20%, T − 2°C and snow + 20%, T + 2°C experiments are very similar to the calculated ELA for the standard run, suggesting that smaller snow depths can be offset by lower temperatures, or vice versa. However, the calculated mass-balance/elevation profiles for the three runs are very different. The warmer, snowier experiment produces a much steeper mass-balance profile than the less snowy, colder run (Fig. 3c, g). Under these warmer, wetter climatic conditions, the glacier would be expected to show a much higher rate of mass throughput than under colder, drier conditions.

TABLE 1

Elevation in meters of $d^2y/dx^2 = 0$ for best-fit cubic polynomials for the 49 sensitivity experiments. S = Winter snow depth; T = Summer temperature. Elevations in bold are those showing the trend discussed in the text.

	S+20%	S+10%	S+5%	S+0%	S−5%	S−10%	S−20%
T−2°C	3309.91	3472.46	3662.79	4177.34	10438.73	1423.18	**2581.75**
T−1°C	3779.90	−10302.79	1830.39	**2413.44**	**2623.05**	**2732.64**	**2844.04**
T−0.5°C	−577.85	**2436.34**	**2620.12**	**2721.64**	**2786.84**	**2832.34**	**2892.74**
T+0°C	**2390.70**	**2702.70**	**2771.08**	**2818.72**	**2853.66**	**2880.68**	**2921.51**
T+0.5°C	**2648.41**	**2792.30**	**2833.41**	**2864.21**	**2888.43**	**2908.36**	**2940.64**
T+1°C	**2741.75**	**2835.61**	**2865.65**	**2889.60**	**2909.36**	**2926.48**	**2955.34**
T+2°C	**2807.38**	**2874.77**	**2898.08**	**2917.66**	**2934.74**	**2950.12**	**2978.47**

TABLE 2

Calculated equilibrium-line altitude for the 49 sensitivity experiments. S = Winter snow depth; T = Summer temperature.

	S+20%	S+10%	S+5%	S+0%	S−5%	S−10%	S−20%
T−2°C	2813	2837	2856	2894	2911	2920	2950
T−1°C	2831	2870	2895	2914	2939	2952	2974
T−0.5°C	2842	2888	2909	2925	2953	2966	2988
T+0°C	2861	2904	2921	2940	2965	2979	3009
T+0.5°C	2890	2917	2940	2955	2975	2992	3023
T+1°C	2908	2935	2952	2969	2986	3013	3034
T+2°C	2946	2969	2981	3007	3019	3039	3091

Discussion

Glacier melt rates depend on the heat fluxes to or from the surface. These, in turn, depend on not only the availability of energy to the surface, but also on the nature of the surface itself, as this will affect the rate of transfer of energy to or from the surface. For turbulent heat fluxes, the key surface condition is the roughness; for radiative fluxes, it is the albedo. For both of these factors, the presence or absence of snow is the primary control on the nature of the surface. Ice surfaces tend to be rougher, and have a lower albedo, than snow surfaces (e.g., Munro, 1990; Brock et al.; 2000b), and thus will melt more quickly under a given set of meteorological conditions. During the course of a melt season, the transient snow line retreats upglacier, exposing rougher, lower albedo ice, which will melt faster than any remaining snow cover. This is one of the fundamental causes of the nonlinear mass-balance profiles found in this study, particularly the reduction in the mass-balance/elevation gradient at higher elevations.

Energy availability also varies over the surface of the glacier. Given the assumptions in the model, turbulent energy availability varies linearly with altitude over the glacier surface (due to the atmospheric lapse rate), and is anyway responsible for only 15% of the total energy flux to the surface (Arnold et al., 1996). Solar radiation, however, provides the largest part of the energy for melting. Figure 4 (solid line) shows the calculated cumulative potential solar radiation, averaged over the glacier surface by 10 m elevation change bands for the modeled melt season. Between ~2550 and ~2800 m, the main tongue of the glacier, potential solar radiation is between 10 and 20% lower than at the very snout of the glacier, or at higher elevations, due to the combination of shading by the high surrounding topography (Mont Collon and the Bouquentins Ridge), plus a northerly aspect. Between 2800 and 2900 m, the potential radiation increases rapidly to a maximum observed value at 2880 m, before reducing gradually (with local fluctuations) until 3100 m. The higher values are due to the more open nature of the upper basin (reducing the impact of shading), lower slope angles and a change in aspect. The rapid decrease in potential radiation at elevations above 3100 m is largely due to the impact of the steep north face of Mont Brule, which accounts for most of the DEM cells at these very high elevations.

The variation in potential solar radiation correlates significantly with the residuals for the best-fit relationship for the standard run ($r = -0.58$) below 3000 m. High potential solar radiation totals are associated with negative mass-balance residuals, and vice versa. The high potential solar radiation values between 2800 and 3000 m would seem to be the *prima facie* cause of the S-shaped mass-balance profile; the pattern of residuals suggesting that the steep mass-balance gradient in this region is due to the higher than expected melt rates in the region of high potential solar radiation. The effect on the mass-balance residuals at high elevations is less marked, however. This would seem to be due to the persistence of high albedo snow throughout the melt season, reducing the importance of solar radiation on the overall surface energy balance here.

The difference between the modeled center-line mass-balance values and the areally averaged values also correlates with the variation in potential solar radiation. Where potential solar radiation values are high (i.e., where shading is relatively unimportant), the difference is small; for areas of lower potential solar radiation, the difference is much more marked.

Ultimately, it is the combination of energy supply to, and absorption by, the surface that will determine the surface melt. Thus, the total *net* solar radiation forms the key control on the surface melt rate, and hence the mass balance. While this is obviously affected by the total potential solar radiation availability, the surface albedo is of crucial importance. Low albedo ice is exposed for longer at lower elevations, leading to higher net solar radiation totals. At higher elevations, low albedo ice is exposed for a shorter period (or not at all), leading to lower net solar radiation totals. This general trend can be seen in Figure 4 (dashed line) for the standard run; this also shows, however, a distinct *reduction* in the rate of decrease of net solar radiation with altitude between ~2750 and ~2900 m; the zone of *increasing* potential solar radiation with elevation. Even though these areas will be snow free for a shorter period, the high solar radiation availability compensates, giving higher net radiation totals. Indeed, there is an obvious positive feedback in operation in this region; high solar radiation will lead to more rapid loss of the snow, reducing the albedo and allowing for more solar radiation to be absorbed. This effect can be seen in the net solar radiation curves for the two most extreme model runs; the snow + 20%, T − 2°C run (dash-dot line) shows a near-continuous decline in net shortwave radiation between 2700 and 2900 m; the snow − 20%, T + 2°C (dotted line) run shows an *increase* in net solar radiation between 2750 and 2800 m, and little decline until above 2900 m. It is this effect which is largely responsible for the change to an increasingly S-shaped mass-balance/elevation profile, and therefore the large observed changes in mass balance at intermediate elevations between the different sensitivity experiments (Fig. 3).

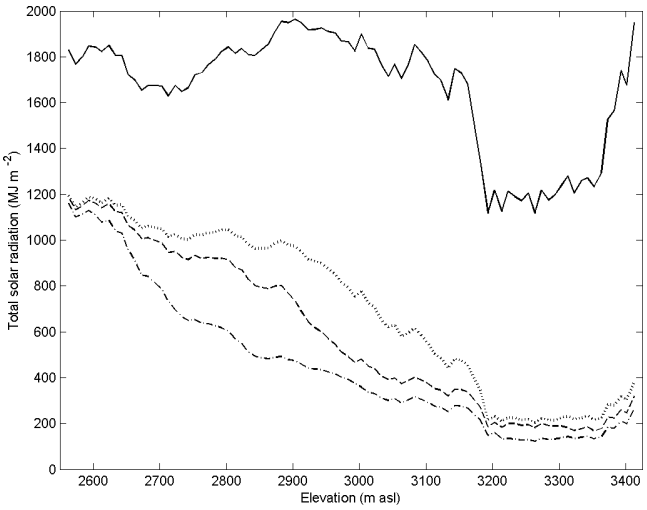

FIGURE 4. Cumulative solar radiation for the modeled time period, averaged over the glacier surface by 10-m elevation-change bands. Solid line: total potential solar radiation; dashed line: net solar radiation for the standard run; dotted line: net solar radiation for the snow − 20%, T + 2°C run; dash-dot line: net solar radiation for the snow + 20%, T − 2°C run.

The variation in potential solar radiation also seems to be the most likely explanation for the different impact of changes in the winter snow depth versus the summer temperature on the mass-balance/elevation profile. Higher snow depths or lower temperatures both lead to a reduction in the length of time that a given elevation will be snow free (or vice versa), and hence will affect the total melt due to the change in net solar radiation, but summer temperature changes will additionally affect the turbulent heat fluxes, which will be higher for the exposed ice surface. Thus, changing winter snow depth has the greatest impact on mass balance at high elevations, where the change in mass balance is almost identical to the change in precipitation as melt rates here are low. At low elevations, the winter snow cover is removed sufficiently quickly that the summer melt rate remains the key determinant of mass balance. Changing summer temperature will affect the melt rate at all elevations, of course, but the effect would be expected to be greater at low elevations, where ice is exposed for longer. For Haut Glacier d'Arolla, however, the increase in potential radiation at intermediate elevations due to more rapid snowline retreat in warmer or drier runs, coupled with the high potential solar radiation

here, makes this zone more sensitive than the snout region itself. At the snout, ice is exposed very quickly due to the generally high melt rates and smaller winter snow depths at lower elevations. As solar radiation supplies 85% of the melt energy, the increase in air temperature in the warmer runs makes little difference to the total amount of melt, as for the bulk of the melt season, low albedo ice is exposed even in the colder runs. This can be clearly seen in Figure 4, where net radiation totals below approximately 2650 m vary only slightly between the three runs shown.

Conclusions

This paper has used a distributed surface energy balance model to explore the sensitivity of the mass-balance/elevation profile of a small valley glacier to different meteorological conditions. The modeled profile for the standard run is best parameterized by a cubic relationship with elevation. This type of relationship successfully captures the change in the gradient of the profile that occurs between low and high elevations, with the mass-balance/elevation gradient decreasing at high elevations due to the lower melt rates. This is caused partly by the lower temperatures, but also by the persistence of snow cover for longer at higher elevations. Residuals from this best-fit relationship correlate strongly with longitudinal changes in potential solar radiation along the glacier. This varies by over 600 MJ m^{-2} due to the complex spatial variability in slope, aspect and shading over the glacier surface.

The complex patterns of solar radiation availability over the glacier surface also lead to differences between modeled center-line mass-balance values, and the modeled average values at different elevation bands. For Haut Glacier d'Arolla, the use of center-line values would lead to total summer melt being over-estimated by more than 8%, compared with areally averaged values. Given the good agreement between modeled melt rates and rates as measured at a series of (center-line) ablation stakes established on the glacier, this suggests that field mass-balance monitoring programs should endeavor to include lateral measurement locations in addition to center-line locations.

Changing summer meteorological and winter snow depth conditions alter not only the mass balance at any given elevation, but also the form of the fitted profile. Warmer summers and reduced winter snowfall lead to an increasingly S-shaped mass-balance/elevation profile, with the largest calculated changes in mass balance occurring at intermediate elevations on the glacier, at or just below the calculated ELA. The high mass-balance sensitivity in these areas leads to very large changes in the calculated ELA between the model runs. The variations in potential solar radiation along the glacier, with high potential radiation totals at intermediate elevations, seem to be the key factor responsible for this sensitivity. The retreat of the summer snowline exposes low albedo ice to high solar radiation totals; if this retreat occurs more rapidly (due to a reduction in winter snow, or increased summer melt), the high potential solar radiation allows large changes in the mass balance to occur. This agrees with the findings of Schmeits and Oerlemans (1997), who found that the response of the mass-balance/elevation profile to climatic change is not independent of altitude, with the largest changes in mass balance occurring at or near the equilibrium line in a 1-dimensional energy balance model for Unterer Grindelwaldgletscher. Using the same model for Franz Joseph Glacier, Oerlemans (1997) also shows that the maximum mass-balance sensitivity occurs just below the equilibrium line, but the overall shape of the mass-balance profile does not alter. In these studies, however, the elevation of peak mass-balance sensitivity does not change; in the experiments reported here, the elevation of maximum mass-balance sensitivity alters as the shape of the mass-balance/elevation profile changes. A fundamental difference between 1-dimensional studies and this one is the inclusion of topographic shading, made possible by the 2-dimensional, distributed model used here, which allows the full impact of the spatial variation in potential solar radiation receipt on mass balance to be accounted for.

In a comprehensive compilation of mass-balance/elevation data from over 80 glaciers, Dyurgerov (2002) also argues that mass-balance/elevation profiles do not simply shift vertically between warmer and colder years; rather, a "rotation" of the mass-balance profile occurs (Dyurgerov 2002: 58), with a resultant change in the mass-balance/elevation gradient. He finds that at high elevations, snow accumulation is the dominant control on mass balance, in agreement with this study. At lower elevations, however, air temperature is the main control, also in agreement with this study, but with the frontal part of the glaciers studied the most sensitive area. For Haut Glacier d'Arolla, this is not the case, because the higher potential solar radiation availability at intermediate elevations on the glacier makes these locations the most sensitive, as discussed above. Again, this shows the importance of the 2-dimensional, distributed approach used in this study.

Incorporating the variability of potential solar radiation over a glacier surface has been found to improve the accuracy of temperature-index models for simulating glacier melt rates (Hock, 1999); the results of this study show that spatial variations in potential solar radiation can also exert a profound control over the form of the mass-balance/elevation profile of a glacier, and how this may change under different meteorological regimes. This, in turn, will strongly affect the response of glaciers to possible future climatic change. The increasing availability of high resolution topographic data should allow more studies of the kind described here to be carried out for a selection of glaciers in different regions, which should in turn improve global estimates of the likely response of glacier mass balance to climatic change.

Acknowledgments

The initial development of the model used in this study was carried out as part of UK Natural Environment Research Council Grant GR3/7004A. A. Gurnell provided the weather station data. Many individuals helped during the 1990 field season, particularly P. Nienow, W. Lawson, B. Hubbard, M. Sharp, and J.-L. Tison, as well as a number of students and volunteers. Grande Dixence S.A. and Y. Bams provided valuable logistic assistance, and M. V. Anzevui granted permission to camp. Subsequent development of the model also occurred under several NERC grants, including GR3/8114 and most recently, GR8/04431.

References Cited

Arnold, N., Willis, I. C. Sharp, M. J., Richards, K. S., and Lawson, W. J., 1996: A distributed surface energy balance model for a small valley glacier: I. Development and testing for Haut Glacier d'Arolla, Valais, Switzerland. *Journal of Glaciology,* 42(140): 77–89.

Braithwaite, R. J. and Olesen, O. B., 1990: A simple energy-balance model to calculate ice ablation at the margin of the Greenland ice sheet. *Journal of Glaciology,* 36(123): 222–228.

Braithwaite, R. and Zhang, Y., 2000: Sensitivity of mass balance of five Swiss glaciers to temperature changes assessed by tuning a degree-day model. *Journal of Glaciology,* 46: 7–14.

Brock, B. W., Willis, I. C., Sharp, M., and Arnold, N. S., 2000a: Modelling seasonal and spatial variations in the surface energy balance of Haut Glacier d'Arolla, Switzerland. *Annals of Glaciology,* 31: 53–62.

Brock, B.W., Willis, I. C., and Sharp, M. J., 2000b: Measurement and parameterisation of albedo variations at Haut Glacier d'Arolla, Switzerland. *Journal of Glaciology,* 46(155): 675–688.

Dyurgerov, M., 2002: Glacier mass balance and regime: Data of measurements and analysis. Meier, M. and Armstrong, R. L. (eds.). *University of Colorado, Institute of Arctic and Alpine Research*

Occasional Paper 55. http://instaar.colorado.edu/other/download/OP55_glaciers.pdf

Escher-Vetter, H., 1985: Energy balance calculations for the ablation period 1982 at Vernagtferner, Oetztal Alps. *Annals of Glaciology,* 6: 158–160.

Hock, R., 1999: A distributed temperature-index ice- and snowmelt model including potential direct solar radiation. *Journal of Glaciology,* 45(149): 101–111.

Hock, R. and Noetzli, C. 1997. Areal melt and discharge modelling of Storglaciaren, Sweden. *Annals of Glaciology,* 24: 211–216.

Laumann, T. and Reeh, N., 1993: Sensitivity to climate change of the mass balance of glaciers in southern Norway. *Journal of Glaciology,* 39(133): 656–665

Munro, D. S., 1990: Comparison of melt energy computations and ablatometer measurements on melting ice and snow. *Arctic and Alpine Research,* 22(2): 153–162.

Munro, D. S. and Young, G. J., 1982: An operational net shortwave radiation model for glacier basins. *Water Resources Research,* 18(2): 220–230.

Oerlemans, J., 1993: A model for the surface balance of ice masses: Part 1. Alpine Glaciers. *Zeitschrift für Gletscherkunde und Glazialgeologie,* 27/28(1991/1992): 63–83.

Oerlemans, J., 1997: Climate sensitivity of Franz Joseph Glacier, New Zealand, as revealed by numerical modelling. *Arctic and Alpine Research,* 29: 233–239.

Oerlemans, J., Anderson, B., Hubbard, A., Huybrechts, Ph., Johannesson, T., Knap, W., Schmeits, M., Stroeven, A. P., van de Wal, R. S. W., Wallinga, J., and Zuo, Z., 1998. Modelling the response of glaciers to climate warming. *Climate Dynamics,* 14: 267–274.

Richards, K. S., Sharp, M., Arnold, N., Gurnell, A., Clark, M., Tranter, M., Nienow, P., Brown, G., Willis, I., and Lawson, W., 1996: An integrated approach to modelling hydrology and water quality in glacierized catchments. *Hydrological Processes,* 10: 479–508.

Schmeits, M. J. and Oerlemans, J., 1997: Simulation of the historical variations in length of Unterer Grindelwaldgletscher, Switzerland. *Journal of Glaciology,* 43(143): 152–164.

Sharp, M., Richards, K., Willis, I., Arnold, N., Nienow, P., Lawson, W., and Tison, J.-L., 1993: *Earth Surface Processes and Landforms,* 18: 557–571.

Walraven, R., 1978: Calculating the position of the sun. *Solar Energy,* 20: 393–397.

Willis, I. C., Sharp, M. J., and Richards, K. S., 1993: Studies of the water balance of Midtdalsbreen, Hardangerjokulen, Norway. I. The calculation of surface water inputs from simple meteorological data. *Zeitschrift für Gletscherkunde und Glazialgeologie,* 27/28(1991/1992): 97–115.

Willis, I., Arnold, N., and Brock, B., 2002: Effect of snowpack removal on energy balance, melt and runoff in a small supraglacial catchment. *Hydrological Processes,* 16: 2721–2749.

Revised ms submitted July 2004